Artigo

A new formulation for predicting the perforation of ballistic impacts in concrete

Uma nova formulação para previsão da perfuração de impactos balísticos em concreto

Thiago Vicente Lima
Letícia dos Santos Aguilera
Suzana Bottega Peripolli
Jose Brant de Campos

Abstract

This work presents a model for determining the depth of projectile perforation based on the RBL formula for ballistic impact, validated with microconcrete specimens made with Portland cement and coarse aggregate of granite and basalt. The model was validated with 7.62 x 51 mm FMJ (Full Metal Jacketed) ammunition on specimens with 5 cm of diameter and a height variation of 5.00 - 10.00 cm The transformation of kinetic energy into heat was found to be one of the forms of energy release. Experimental results showed that the calculation model proposed here predicts penetration depth values closer to the experimental values than current models, which is favorable for the safety.

Keywords: concrete constitutive model. Ballistic impact. Microconcrete.

[1]**Thiago Vicente Lima**
[1]Universidade do Estado do Rio de Janeiro
Rio de Janeiro - RJ - Brazil

[2]**Letícia dos Santos Aguilera**
[2]Universidade do Estado do Rio de Janeiro
Nova Friburgo - RJ - Brazil

[3]**Suzana Bottega Peripolli**
[3]Universidade do Estado do Rio de Janeiro

[4]**Jose Brant de Campos**
[4]Universidade do Estado do Rio de Janeiro
Rio de Janeiro - RJ - Brazil

Recebido em 15/05/23
Aceito em 14/08/23

Resumo

Este trabalho apresenta um modelo para determinar a profundidade da penetração de um projetil baseado sobre a formula RBL para impactos balísticos, validados com corpos de prova de microconcreto feito em cimento Portland, agregados de granitos grossos e basalto. O modelo foi validado com munição FMJ (revestido totalmente de metal) de 7,62 x 51 mm sobre corpos de prova de 5 cm de diâmetro e alturas variando entre 5 a 10 cm. Foi possível determinar que uma das formas de liberação de energia ocorreu a través da energia cinética em calor. Os resultados experimentais mostram que o modelo calculado aqui predisse valores de profundidade de penetração mais próximos aos valores experimentais usados nos modelos atuais, das quais são favoráveis para a segurança.

Palavras-chave*: Modelo constitutive de concreto. Impacto balístico. Microconcreto.*

Introduction

Concrete is widely used in civil construction, with many applications that utilize its inherent qualities. Its use as a ballistic protection material is valid, as it has been used by military and civil engineers for many years in the construction of protective structures, such as bunkers, wooded houses and lockers in order to resist impacts of explosives. Several studies have demonstrated the effectiveness of concrete in this application, with good results as reported in many studies (Chen *et al.*, 2023; Gao; Kong; Fang, 2023; Xin *et al.*, 2023; Sun *et al.* 2021; Rajput; Iqbal; Gupta, 2018; Tu; Lu, 2010; Li *et al.*, 2005; Teng *et al.*, 2005). However, the mechanical forces of penetration and perforation of concrete are more complex than in metals, due to its distinct behavior under compressive and tensile forces. Therefore, the study of concrete as a ballistic protection material must consider these complex forces during impact (Rajput; Iqbal, 2017; Abdel-Kader; Fouda, 2014; Wu; Chen; Zhang, 2015). Besides, many studies also describe the complex interplay of factors involved in the reactions of concrete to impact, such as the combination of inertia effects, material loading speed, and the form of energy propagation.

Concrete is a composite material~~,~~ composed of a variety of heterogeneous materials. When subjected to dynamic loads, it undergoes catastrophic fracture, with multiple fragmentation and pulverization. The process starts with the initial elastic response of the material, followed by plastic flow, micro- and macro-crack formation, fragmentation, and finally rupture (Grote; Park; Zhou, 2001).

Zielinski and Reinhardt (1982) found that the uniaxial-generated tensile impact strength of microconcrete and common concrete is greater than that of mortar. This can be explained by the interruption of cracks by coarse aggregate particles, which are harder and denser than the matrix. The crack interruption increases the amount of energy absorbed in the fracture process. Ozbek *et al.* (2013) observed that cracks in concrete form parallel to the loading axis, followed by shear cones below the aggregates. They also observed that the fracture does not only occur in the cement paste, but also propagates through the aggregates. Micallef *et al.* (2014) and Du, Jin and Ma (2014) found that shear mechanisms generally govern the behavior of reinforced concrete structures subjected to localized impact loads. Garcia-Avila, Porta Nova and Rabiei (2014) described how the impact face material can decelerate, degrade, and erode the projectile.

Polanco-Loria *et al.* (2008) reported that modeling and formulations can be used to describe the effect of loading on concrete by projectiles. Li *et al.* (2005) reviewed a number of formulations that have been used to try to understand the effect of projectiles impact, with the goal of predicting damage and perforation depth.

The continuous improvement of weapons and projectiles has required the constant development of materials and protective structures for the protection of human life, as shown in the studies by Andraskar, Tiwari and Goel (2022) and Wu *et al.* (2020).

Firearms that were once used for hunting and warfare are now commonly used by criminals and terrorists. This has led to a need for improved protection for civilians, including their homes, buildings, and guardhouses. Several authors have studied the use of large-caliber weapons, such as the 7.62 x 51 mm, in attacks against these structures (Iqbal *et al.*, 2023; Dresch *et al.*, 2021; Choudhary *et al.*, 2020; Chao *et al.*, 2019; Polla *et al.*, 2019).

For that reason, in this study is propose and evaluate a new model of the United States Army Corps of Arms (ACA) formulation for microconcrete with impacts of 7.62 mm projectiles on concrete specimens confined with basalt or granite as aggregate, and assesses its interferences.

Proposed analytical structural model

The adapted formula (Equation 1) from the Ballistics Research Laboratory (LRB) of the ACA, cited by Li *et al.* (2005), is the most widely used security prediction model:

$$\frac{x}{d} = \frac{1.33\times10^{-3}}{\sqrt{f_c}}\left(\frac{M}{d^3}\right) d^{0.2} V_0^{1.33} \qquad \text{Eq. 1}$$

Several authors have used this formula as a basis for their models (Wu; Chen; Zhang, 2015; Ben-Dor; Dubinsky; Elperinet, 2009; Vossoughi *et al.*, 2007).

The kinetic energy of a 7.62 mm rifle shot is almost constant, as its mass is the same in all shots and the speed will be between 800 to 850 m/s. This energy (E) directly influences the projectile's penetration. In the modification proposed in the present study, the initial kinetic energy (E) is introduced into the square root of Equation 1 and divided by the material strength.

This hypothesis is plausible because material strength is inversely proportional to penetration, and material strength (f) and impact energy (E) are associated factors.

This formulation raises the velocity variation (V_0) to 1.33 instead of squaring it (2). This reduces the direct influence of the velocity factor, thus emphasizing the initial energy term (E). This also considers the pressure loss on impact to the medium that is not absorbed in the bulkhead system. In this new proposal, the term $\sqrt{fc}$ in Equation 1 is replaced by $\sqrt{E/f_c}$.

The numerical factor of Equation 1 (1.33×10^{-3}) was altered by incorporating the minimum thickness of scabbing displacement, where hs/d = 2x/d.

Therefore, the final protection value of the plate against scattering or subsequent detachment of fragments from the face opposite to the trip can be predicted without the need for a second calculation.

The effective perforation will be e/d = 1.3x/d.

The new factor will be incorporated into the final value of the formula, which will be determine the minimum thickness of the plate required to stop the projectile without the displacement.

The factor contained in the proposed new formula is the result of multiplying the existing constants from previous modifications (2 x 1.3 = 2.6).

Taking into account an initial factor with a safety range of 15% to cover the resistance variation of the same slab of the same material due to the heterogeneities of the concrete, we have 2.6 x 1.15 = 2.99. Therefore, the final constant is suggested to be 3.0.

Equation 2 presents the proposed modeling, called "Vicente Lima":

$$\frac{x}{d} = \frac{3.00\times10^{-2}}{\sqrt{E/fc}}\left(\frac{M}{d^3}\right) d^{0.2} V_0^{1.33} \quad \text{Eq. 2}$$

Experimental procedures

Experimental tests were conducted to characterize the material under study and validate the Vicente Lima model in real-world settings.

Compression test

Concrete based on Portland cement composite with the addition of granulated blast furnace slag (CPII-E-40 RS), manufactured by MIZU SA, was dosed with proportions of gravel of zero grade (granite or basalt) for production of specimens for the tests. The volume of gravel was kept constant as a reference, and the same washed sand, commercialized in the region, from the Guandu River (Rio de Janeiro – RJ – Brazil), was used for all samples (Figure 1).

The specimens were molded with dimensions of ∅ 5 cm of diameter and height of 5 cm for the preliminary ballistic impact tests (two specimens), as shown by RAJPUT *et al.* (2018), and ∅ 5 cm of diameter and height of 10 cm for the ballistic impact resistance tests (two copies) and compressive strength (three copies), as suggested by Rajput and Iqbal (2017), see Figure 2. Micro-concrete was used to prevent the wall effect from occurring during molding due to the low ratio of mold size to maximum aggregate dimension.

The compressive strength test on specimens of ∅ 5 cm x 10 cm were conducted in accordance with the recommendations of NBR 5739 (ABNT, 2018). The results are presented in Table 1.

Gabet, Malécot and Daudeville (2008) worked with fine aggregate concretes with a maximum aggregate diameter of 8 mm, and achieved results close to 30 MPa. This demonstrates that the type of aggregate influences the strength of concrete, as also shown by other studies (Gao *et al.*, 2020; Kazemian; Rooholamini; Hassani, 2019; Werner; Thienel; Kustermann, 2013; Pacheco-Torgal *et al.*, 2007; Donza; Cabrera; Irassar, 2002).

Ballistic impact

Ballistics tests were conducted at the Army Assessment Center - CAEx (Rio de Janeiro - RJ - Brazil), in the Test Line for Small Arms - Line IV, with 7.62 x 51 FMJ (Full Metallic Jacket) projectiles with a mass of 9.8 g and a shooting stand, according to the experimental setup shown in Figure 3. The shielding system's protection level against ballistic impact, according to NBR 15000 (ABNT, 2020), is presented in Table 2.

Figure 1 - **Coarse aggregate, gravel grade 0# (zero) (a) Granite and (b) Basalt**

(a) (b)

Figure 2 - **(A) Molds used; (B) Cylindrical specimens (∅□5 cm x 5 cm) and (∅□5 cm x 10 cm); e (C) Specimens in wet curing in drinking water for 28 days**

(a) (b) (c)

Table 1 - **Compressive strength test specimens in Ø5 x 10cm**

Compressive strength test (MPa) 28 days		
	Aggregate	
	Granite	Basalt
Specimens	19.86	36.87
	35.60	35.24
	25.46	37.89
Average	26.98	36.67
Standart deviation	7.98	1.34

Figure 3 - **Stand, side view (Line IV-CAEx)**

Table 2 – **Ammunition used in ballistics tests: level and type**

Level	Ammunition	Mass of the Projectile (g)	V_0 (m/s)	Impact Energy (J)
III	7.62 x 51FMJ (.308 – Winchester)	9.8 ± 0.1	838 ± 15	3.406

Source: NBR 15000 (ABNT, 2020).

Note: FMJ – Full Metal Jacketed.

The confinement and anchoring system for the specimens was created using the cylindrical specimen molding forms. These consist of a cylindrical body cut along its generatrix, with a thread at the lower end. To resist the expansion effort of the concrete, the cylindrical body has a steel clamp with a nut and lock nut welded to it, which is closed by a steel T-bolt. Two of these pieces were joined together by a steel sleeve, with the addition of a 1 mm thick aluminum sheet at the front end (Figure 4).

A device with a height of 20 cm and an internal diameter of 5 cm was used for specimens (CP) with two different heights, 5 and 10 cm. The device is similar to that used by Zhang *et al*. (2019), and square plates with a side of 5 cm have also been used in the literature (Fabris *et al.*, 2020). The specimens were confined in the molds themselves to better understand the reaction of the materials to the impact of the projectile and its shock wave.

The PCs were anchored to the ballistic test fixture, which had a metal plate with good resistance to perforation as the bottom shield (see Figure 5). Test results are shown in Table 3 and 4.

Although all ∅5 x 5 cm CPs failed to retain the projectile, the anchoring mechanism of the system was found to be valid. In the reference plate, it was observed that concrete strength did not influence the result due to the low thickness of the CP. However, the type of aggregate, with different grain formats, helped to minimize the damage caused to the plate.

Granite has a more rounded shape with a rougher surface, while basalt has a lamellar shape with a smoother surface. This difference in grain shape was reflected in the damage to the reference plates at the bottom of the CPs. The granite CPs did not suffer visible damage, while the basalt CPs had the mark of the projectile's collision well defined.

The tests with ∅5 x 10 cm CPs were anchored on the device, as shown in the results in Table 4. Figure 6 shows that the confinement system resisted the impact of the projectile and retained the test specimen inside. The confinement form remained in good condition.

The loss of mass is proportional to the perforation, as shown in Table 4. The reason for this behavior is because the specific kinetic energy (initial kinetic energy of the projectile per unit of concrete compressive strength) is proportional to both the loss of mass and perforation. This means that we can use the specific kinetic energy to obtain a reference value constant for the loss of mass and the perforation. The penetration depth is calculated from the initial and final height difference of the CP.

Comparison of the analytical model with the experimental result

Figure 7 shows a graph comparing the actual impact effect, the LRB formula (Equation 1), and the Vicente Lima formula. The specific kinetic energy is plotted on the x-axis, relative to the material's resistance, and the perforation reached by the projectile or expected is plotted on the y-axis.

Use numerical simulations to validate or predict the response of the impacted object (Kamran; Iqbal, 2022; Wang; Guo; Hou, 2022; Rajput; Iqbal; Bhargava, 2017; Morales-Alonso *et al.*, 2015; Jinzhu *et al.*, 2013; Park; Yoo; Chungb, 2005).

The input data on the ordinate axis, using the relationship between strength and impact energy, highlights a common behavior among the materials, with the formation of groups by type of materials. This makes the visualization of depth evident for each group. In addition, it reduces distortions in energy variation and compensates for the resistance of the material used, which is provided by the average.

Table 5 shows that the adaptation of the original formula led to results that were closer to the depth generated by the impact for the two aggregates. The values of the empirical formulas were compared to the real value, and the negative values are more favorable as a safety factor, with a predicted penetration that is greater than the actual penetration.

Figure 4 - **(a) Parts of the containment device; (b) Assembled device; e (c) Sample confined in the device**

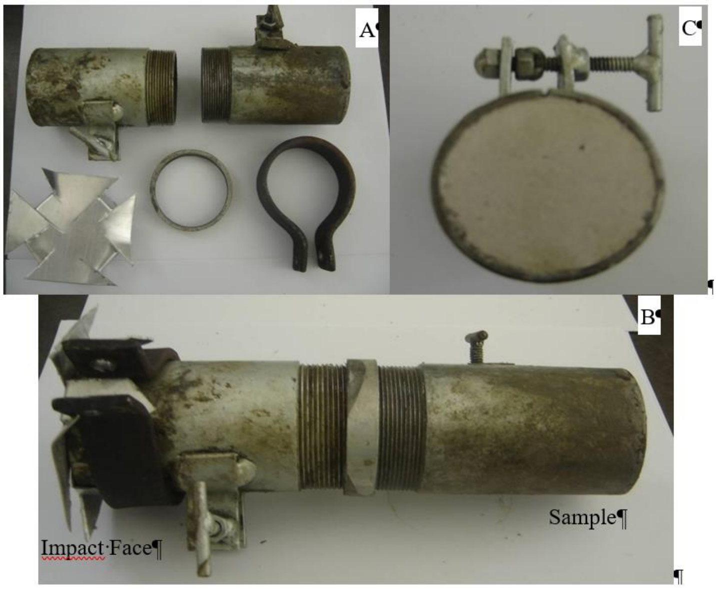

Figure 5 - **Bulkhead with ∅5 x 5cm (diameter x height) specimen, before and after shooting to the left and right, respectively. The projectile mark can be observed on the concrete set on the plate**

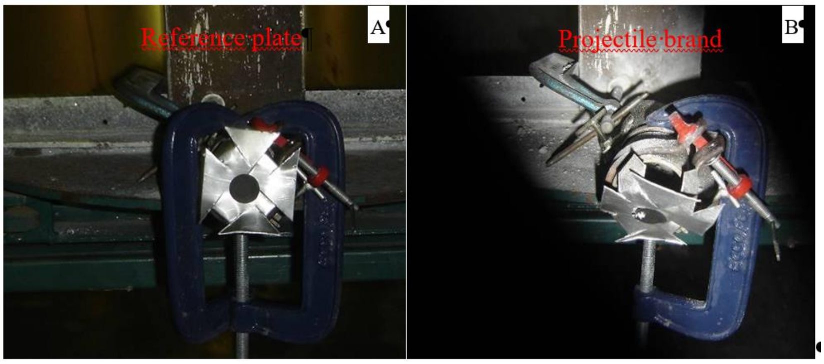

Table 3 - **Mass loss of ∅5 x 5 cm concrete specimens after impact test**

Specimen	Initial Mass (g)	Final Mass (g)	Initial Height (cm)	Final Height (cm)	Velocity (m/s)	Impact Energy (J)	NP
Basalt	244.34	0.00	5.20	0.00	836.00	3424.59	PC
	254.62	0.00	5.15	0.00	829.00	3367.48	PC
Granite	236.50	0.00	5.00	0.00	842.00	3473.92	PC
	230.28	0.00	5.20	0.00	838.00	3440.99	PC

Note: NP: Drilling Level; and
PC: Full Penetration.

Table 4 - **Mass loss of ∅5 x 10 cm concrete specimens after impact test**

Specimen	Initial Mass (g)	Final Mass (g)	Initial Height (cm)	Final Height (cm)	Velocity (m/s)	Impact Energy (J)	NP
Basalt	443.11	209.19	10.14	4.52	839.00	3449.21	PP
	448.29	213.68	10.13	4.38	837.00	3432.79	PP
Granite	443.48	221.34	9.96	5.77	833.00	3400.06	PP
	443.42	218.26	9.86	5.75	835.00	3416.40	PP

Note: NP: Drilling Level; and
PP: Partial Penetration.

Figure 6 - **Specimen inside the mold after firing**

Figure 7 - **The relationship between specific kinetic energy and compressive strength can be used to predict penetration depth (*5.00 cm height)**

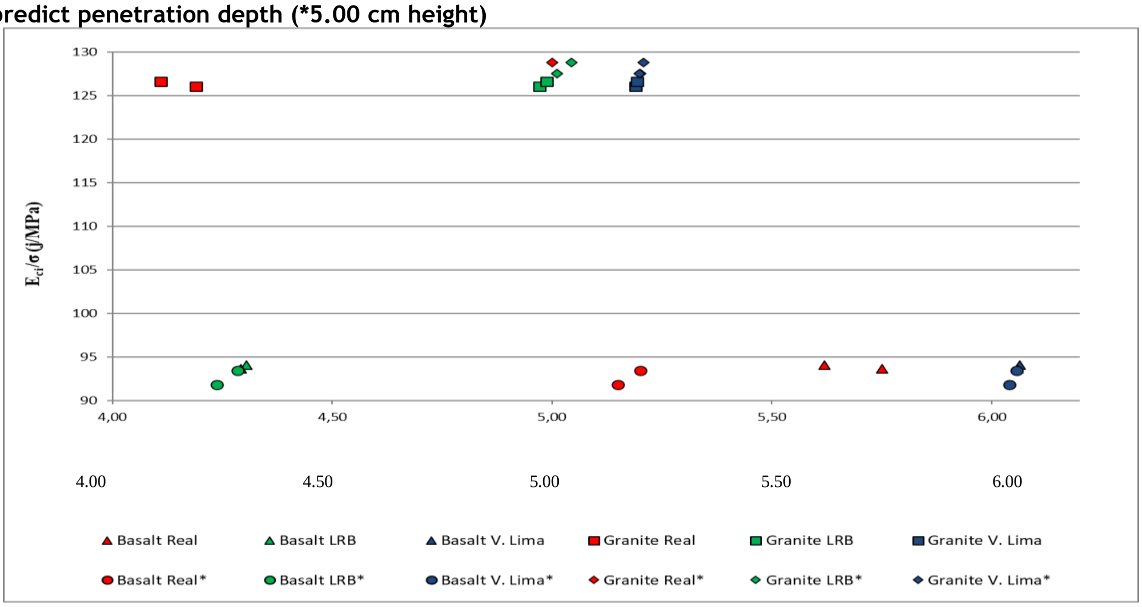

Table 5 - **Penetration results, simulations, and percentage difference**

Real and Calculated penetration (cm)					
Specimen	**Real**	**RLB**	**%**	**V. Lima**	**%**
Basalt	5.62	4.31	23.39%	6.06	-7.89%
	5.75	4.29	25.36%	6.06	-5.37%
Granite	4.19	4.97	18.65%	5.19	-23.84%
	4.11	4.99	21.35%	5.19	-26.35%
Basalt*	5.20	4.28	17.60%	6.06	-16.47%
	5.15	4.24	17.72%	6.04	-17.27%
Granite*	5.00	5.04	-0.86%	5.21	-4.14%
	5.20	5.01	-3.63%	5.20	0.19%

As shown in Table 5, the Vicente Lima formula predicts a minimum final thickness of the protection layer with a good safety margin. All results were higher than the real impact values, which is favorable for security and defense. When compared to the RLB formula (Equation 1), these values provide a comfortable safety value and a dimension that is much closer to the real impact, allowing for a better design of the protection bulkhead.

Conclusion

The restructuring of the values of the original LRB formula (1941) from the US Army Weapon Corps provided a better dimensioning of the impact damage in terms of actual depth for microconcrete. It also presented a better penetration value and a safety factor already included in the prediction of the minimum plate thickness.

From the results of the impact tests, we can conclude that the height of 5 cm specimens did not resist the impact, as predicted by the new formulation. The heights of 10 cm specimens were able to stop the projectile and retain part of its body. In this case, the influence of the safety factor is clear, as the remaining part is greater than the CP forecast and the calculated value.

The concrete strength does not directly correlate with the damage caused, but the aggregate type is more significant. This is evident in the Vicente Lima formula, which better approximates the real results for granite aggregate.

The type of aggregate has a direct influence on the resistance and rupture models. Granitic aggregates, which are rougher and rounder, tend to conical rupture, while basaltic aggregates, which are more lamellar, tend to planar rupture.

References

ABDEL-KADER, M.; FOUDA, A. Effect of reinforcement on the response of concrete panels to impact of hard projectiles. **International Journal of Impact Engineering**, v. 63, p. 1-17, 2014.

ANDRASKAR, N. D.; TIWARI, G; GOEL, M. D. Impact response of ceramic structures: a review. **Ceramics International**, V. 48, p. 27262–27279, 2022.

ASSOCIAÇÃO BRASILEIRA DE NORMAS TÉCNICAS. **NBR 15000**: blindagens para impactos balísticos: classificação e critérios de avaliação. Rio de Janeiro, 2020.

ASSOCIAÇÃO BRASILEIRA DE NORMAS TÉCNICAS. **NBR 5739**: (MB3): concreto: ensaio de compressão de corpos-de-prova cilíndricos. Rio de Janeiro, 2018.

BEN-DOR, G.; DUBINSKY, A.; ELPERINET T. Ballistic properties of multilayered concrete shields. **Nuclear Engineering and Design**, v. 239, p. 1789–1794, 2009.

CHAO, Z. L. *et al.* The microstructure and ballistic performance of B4C/AA2024 functionally graded composites with wide range B4C volume fraction. **Composites Part B**, v. 161, p. 627–638, 2019.

CHEN, Z. *et al.* Numerical study of fractal analysis of crack propagation in concrete under different strain rates by mesoscale particle element modeling. **International Journal of Impact Engineering**, v. 173, p. 1–9, 104440, 2023.

CHOUDHARY, S. *et al.* Ballistic impact behaviour of newly developed armour grade steel: An experimental and numerical study. **International Journal of Impact Engineering**, v. 140, p. 1–10, 103557, 2020.

DONZA, H.; CABRERA, O.; IRASSAR, E. F. High-strength concrete with different fine aggregate. **Cement and Concrete Research**, v. 32, p. 1755–1761, 2002.

DRESCH, A. B. *et al.* Ballistic ceramics and analysis of their mechanical properties for armour applications: a review. **Ceramics International**, V. 47, p. 8743–8761, 2021.

DU, X.; JIN, L.; MA, G. Numerical simulation of dynamic tensile-failure of concrete at meso-scale. **International Journal of Impact Engineering**, v. 66, p. 5–17, 2014.

FABRIS, D. C. N. *et al.* Effect of MgO·Al2O3·SiO2 glass-ceramic as sintering aid on properties of alumina armors. **Materials Science & Engineering A**, v. 781, p. 1–13, 139237, 2020.

GABET, T.; MALÉCOT, Y.; DAUDEVILLE, L. Triaxial behaviour of concrete under high stresses: Influence of the loading path on compaction and limit states. **Cement and Concrete Research**, v. 38, p. 403–412, 2008.

GAO, C. *et al.* Mechanical properties of recycled aggregate concrete modified by nano-particles. **Construction and Building Materials**, v. 241, p. 1–15, 118030, 2020.

GAO, C.; KONG, X.; FANG, Q. Experimental and numerical investigation on the attenuation of blast waves in concrete induced by cylindrical charge explosion. **International Journal of Impact Engineering**, v. 174, p. 1–19, 104491, 2023.

GARCIA-AVILA, M.; PORTANOVA, M.; RABIEI, A. Ballistic performance of a composite metal foam-ceramicarmor system. **Procedia Materials Science**, v. 4, p. 151–156, 2014.

GROTE, D. L.; PARK, S. W.; ZHOU, M. Dynamic behavior of concrete at high strain rates and pressures: I. experimental characterization. **International Journal of Impact Engineering**, v. 25, p. 869–886, 2001.

IQBAL, M. *et al.* Development of mortar filled honeycomb sandwich panels for resistance against repeated ballistic impacts. **Journal of Materials Research and Technology**, v. 24, p. 8121–8134, 2023.

JINZHU, L. *et al.* Perforation experiments of concrete targets with residual velocity measurements. **International Journal of Impact Engineering**, v. 57, p. 1-6, 2013.

KAMRAN, K.; IQBAL, M. A. The ballistic evaluation of plain, reinforced and reinforced–prestressed concrete. **Thin-Walled Structures**, v. 179, 109707, 2022.

KAZEMIAN, F.; ROOHOLAMINI, H.; HASSANI, A. Mechanical and fracture properties of concrete containing treated and untreated recycled concrete aggregates. **Construction and Building Materials**, v. 209, p. 690–700, 2019.

LI, Q. M. *et al.* Local impact effects of hard missiles on concrete targets. **International Journal of Impact Engineering**, v. 32, p. 224–284, 2005.

MICALLEF, K. *et al.* Assessing punching shear failure in reinforced concrete flat slabs subjected to localised impact loading. **International Journal of Impact Engineering**, v. 71, p. 17-33, 2014.

MORALES-ALONSO, G. *et al.* Influence of the softening curve in the fracture patterns of concrete slabs subjected to blast. **Engineering Fracture Mechanics**, v. 140, p. 1–16, 2015.

OZBEK, A. S. A. *et al.* Dynamic behavior of porous concretes under drop weight impact testing. **Cement & Concrete Composites**, v. 39, p. 1–11, 2013.

PACHECO-TORGAL, F.; CASTRO-GOMES, J.; JALALI S. Investigations about the effect of aggregates on strength and microstructure of geopolymeric mine waste mud binders. **Cement and Concrete Research**, v. 37, p. 933–941, 2007.

PARK, M.; YOO, J.; CHUNGB, D. T. An optimization of a multi-layered plate under ballistic impact. **International Journal of Solids and Structures**, v. 42, p. 123–137, 2005.

POLANCO-LORIA, M. *et al.* Numerical predictions of ballistic limits for concrete slabs using a modified version of the HJC concrete model. **International Journal of Impact Engineering**, v. 35, p. 290–303, 2008.

POLLA, M. *et al.* Ballistic performance of multilayer structures based on alumina/epoxy. **Cerâmica**, v. 65, p. 207–215, 2019.

RAJPUT, A.; IQBAL, M. A.; BHARGAVA, P. Experimental and numerical study of concrete targets under high rate of loading. **Procedia Engineering**, v. 173, p. 130–137, 2017.

RAJPUT, A.; IQBAL, M. A. Ballistic performance of plain, reinforced and pre-stressed concrete slabs under normal impact by an ogival-nosed projectile. **International Journal of Impact Engineering**, v. 110, p. 57–71, 2017.

RAJPUT, A; IQBAL, M. A.; GUPTA, N. K. Ballistic performances of concrete targets subjected to long projectile impact. **Thin-Walled Structures**, v. 126, p. 171–181, 2018.

SUN, S. *et al.* The composite damage effects of explosion after penetration in plain concrete targets. **International Journal of Impact Engineering**, v. 153, p. 1–11, 103862, 2021.

TENG; T. L. *et al.* Penetration resistance of reinforced concrete containment structures. **Annals of Nuclear Energy**, v. 32, p. 281–298, 2005.

TU, Z.; LU, Y. Modifications of RHT material model for improved numerical simulation of dynamic response of concrete. **International Journal of Impact Engineering**, v.37, p. 1072-1082, 2010.

VOSSOUGHI, F. *et al.* Resistance of concrete protected by fabric to projectile impact. **Cement and Concrete Research**, v. 37, p. 96–106, 2007.

WANG, Z. Y.; GUO, Q. Q.; HOU, C. C. Numerical study on the ballistic performance of prestressed concrete slabs subjected to hard missile impact. **International Journal of Impact Engineering**, v. 168, p. 1–18, 104318, 2022.

WERNER, S.; THIENEL, K. C.; KUSTERMANN, A. Study of fractured surfaces of concrete caused by projectile impact. **International Journal of Impact Engineering**, v. 52, p. 23-27, 2013.

WU, K. K. *et al.* Ballistic impact performance of SiC ceramic-Dyneema fiber composite materials. **Advances in Materials Science and Engineering**, v. 2020, 9457489, p. 1–9, 2020.

WU, M.; CHEN Z.; ZHANG C. Determining the impact behavior of concrete beams through experimental testing and meso-scale simulation: I: drop-weight tests. **Engineering Fracture Mechanics**, v. 135, p. 94–112, 2015.

XIN, B. *et al.* Experimental study of deep-burial underground structures subjected to multiple 45◦ side–top far-field explosions. **International Journal of Impact Engineering**, v. 173, p. 1–20, 104432, 2023.

ZHANG, R. *et al.* Influence of prestress on ballistic performance of bi-layer ceramic composite armors: Experiments and simulations. **Composite Structures**, v. 227, p. 1–10, 111258, 2019.

ZIELINSKI, A. J.; REINHARDT, H. W. Stress-strain behaviour of concrete and mortar at high rates of tensile loading. **Cement and Concrete Research**, v. 12, n. 3, p. 309-319, 1982.

Thiago Vicente Lima
Research, Methodology, Writing of the original manuscript.

Mechanical Engineering Department | Universidade do Estado do Rio de Janeiro | Rua Fonseca Teles, 121, São Cristovão | Rio de Janeiro – RJ – Brazil | CEP 20940-200 | Tel.: (21) 2332-4736 | E-mail: thigocivil@yahoo.com

Letícia dos Santos Aguilera
Supervision, Writing – review & editing.

Polytechnic Institute | Universidade do Estado do Rio de Janeiro | Nova Friburgo – RJ – Brazil | CEP 28625-570 | Tel.: (22) 2533-2263 | E-mail: leticia.aguilera@iprj.uerj.br

Suzana Bottega Peripolli
Supervision, Writing – review & editing.

Mechanical Engineering Department | Universidade do Estado do Rio de Janeiro | Tel.: (21) 2332-4736 | E-mail: speripolli@gmail.com

Jose Brant de Campos
Conceptualization, Administration of project, Supervision, Writing – review and editing.

Mechanical Engineering Department | Universidade do Estado do Rio de Janeiro | Rua Fonseca Teles, 121, São Cristovão | Rio de Janeiro – RJ – Brazil | CEP 20940-200 | Tel.: (21) 2332-4736 | E-mail: brant@uerj.br

Editor: **Marcelo Henrique Farias de Medeiros**

Editoras de seção: **Ercília Hitomi Hirota** e **Juliana Parise Baldauf**

Ambiente Construído
Revista da Associação Nacional de Tecnologia do Ambiente Construído
Av. Osvaldo Aranha, 99 - 3º andar, Centro
Porto Alegre – RS - Brasil
CEP 90035-190
Telefone: +55 (51) 3308-4084
www.seer.ufrgs.br/ambienteconstruido
www.scielo.br/ac
E-mail: ambienteconstruido@ufrgs.br